

Magnetic Bead-Guided Assembly of 3D Primary Human Islet Cells in Decellularized Pancreatic Scaffolds

Marluce da Cunha Mantovani ^{1,2}, Ana Claudia Oliveira Carreira ¹, Nilsa Regina Damaceno-Rodrigues ³, Elia Garcia Caldini ³ and Mari Cleide Sogayar ^{1,4,*}

¹ Cell and Molecular Therapy NUCEL Group, School of Medicine, University of São Paulo, Av. Dr. Arnaldo, 455, São Paulo 01246-903, SP, Brazil; marluce@usp.br (M.d.C.M.); ancoc@iq.usp.br (A.C.O.C.)

² Technical Division for Teaching, Research and Innovation Support—(DTAPEPI) Biotechnology and Innovation Facility, School of Medicine, University of São Paulo, São Paulo 01246-903, SP, Brazil

³ Laboratory of Cell Biology, Department of Pathology, School of Medicine, University of São Paulo, São Paulo 01246-903, SP, Brazil; nilsa@usp.br (N.R.D.-R.); elia@usp.br (E.G.C.)

⁴ Biochemistry Department, Chemistry Institute, University of São Paulo, São Paulo 05508-900, SP, Brazil

* Correspondence: mcsoga@iq.usp.br; Tel.: +55-(11)-3061-8102 or +55-(11)-99204-2844

Abstract

Background: Three-dimensional (3D) cell cultures are increasingly recognized as effective models for studying diseases and developing cell therapies. In the endocrine pancreas field, organoids/spheroids derived from human islet cells enable advances in diabetes research, drug screening, and tissue engineering. While various 3D culture methods exist, approaches such as magnetic bead-assisted aggregation remain underexplored for endocrine pancreatic cells. Additionally, the use of biological scaffolds, especially those derived from decellularized pancreatic extracellular matrix, provides a biomimetic environment that promotes adhesion, proliferation, and functionality of pancreatic cells. This study presents a protocol for magnetic bead-guided 3D culture of human islet cells within decellularized pancreatic scaffolds. **Methods:** Human pancreas from adult brain-dead donors was harvested for both islets' isolation processing and decellularization to generate an acellular pancreatic bioscaffold. Primary human pancreatic islets were first grown in two-dimensional adherent cultures, then enzymatically harvested from the surface and reassembled into three-dimensional clusters using different initial cell amounts (small clusters 0.5×10^4 – 1×10^4 and larger clusters 2.5×10^4 – 5×10^4 cells) and then placed within acellular pancreatic slices of different thickness, namely 50 and 90 μm . Optic microscopic examination, scanning electron microscopy analysis, and assessment of insulin and lactate dehydrogenase (LDH) levels were used to evaluate these 3D islet-like cluster cultures. **Results:** We report the establishment of 3D cultures derived from primary pancreatic islet cells using a magnetic approach in a remarkable 18 h period for the complete formation of 3D clusters. The small clusters (0.5×10^4 – 1×10^4 cells) exhibited a faster attachment to the acellular matrix, with cells visibly spreading outside the cluster interacting with the bioscaffold slice, when compared to the larger clusters (2.5×10^4 – 5×10^4 cells). These cells continued to produce insulin, and no statistically significant differences in LDH levels were found under these different conditions. **Conclusions:** Here, we demonstrate that a magnetic bead-based protocol can be successfully applied to endocrine pancreatic cells, enabling the rapid formation of compact, viable, and functional 3D structures. Despite limitations such as higher cost and prolonged retention of magnetic particles, the approach supports size-dependent interactions with decellularized pancreatic scaffolds. These findings are valuable for researchers designing experiments tailored to specific objectives and underscore the potential of this platform for advancing diabetes research and pancreatic tissue engineering.



Academic Editor: Thierry Coppola

Received: 18 June 2025

Revised: 2 February 2026

Accepted: 3 February 2026

Published: 7 February 2026

Copyright: © 2026 by the authors.

Licensee MDPI, Basel, Switzerland.

This article is an open access article distributed under the terms and

conditions of the [Creative Commons](https://creativecommons.org/licenses/by/4.0/)

[Attribution \(CC BY\)](https://creativecommons.org/licenses/by/4.0/) license.

Keywords: human pancreas; 3D islet cells cultures; pancreatic islet organoids; spheroids; decellularized pancreas

1. Introduction

Three-dimensional (3D) culture systems have become essential tools in regenerative medicine and disease modeling, especially since they provide a closer approximation of the *in vivo* microenvironment compared to traditional two-dimensional (2D) cultures [1]. Among these, organoid and spheroid models have been extensively explored due to their capacity for self-organization, maintenance of phenotypic traits, and responsiveness to external stimuli. In the endocrine pancreas field, 3D systems derived from human islets, embryonic progenitors, or pluripotent stem cells have demonstrated great potential for disease modeling, drug screening, and future cell therapy approaches [2–5].

Numerous strategies have been explored to enable three-dimensional (3D) cell culture systems, which better mimic the *in vivo* physiological microenvironment. Commonly used techniques include (a) hanging drops cell cultures [6], (b) using rotating cell culture systems or low-attachment plastics surfaces [6], (c) pyramid-shaped plates containing conical wells [7], (d) scaffold-free hydrogels [8], (e) macroporous scaffolds [9], and (f) magnetic beads systems [10]. The hanging drops method, while widely adopted, presents limitations such as low scalability, labor-intensive handling, and challenges in medium replacement and compound addition. Furthermore, not all cell types are able to form compact spheroids using this approach [6]. Suspension cultures using non-adhesive substrates or rotational agitation promote spheroid formation but are associated with size heterogeneity, mechanical stress, and limited longevity of cultures [6]. Pyramid well plates offer standardized spheroid dimensions but are expensive and may be difficult to handle [7]. Scaffold-free hydrogel provides significant advantages, including the ability to precisely regulate the size of 3D constructs and produce a large quantity per plate. In this approach, cells are seeded into a hydrogel containing preformed wells, where they settle and spontaneously assemble into 3D spheroids [8]. Macroporous scaffolds often suffer from inconsistent cell seeding due to variable pore sizes, requiring additional engineering strategies to improve distribution [9]. Magnetic bead-based aggregation allows targeted cell organization, but the method is costly and may result in intracellular nanoparticle retention [10].

Regarding pancreatic endocrine cells, especially islet-derived cultures, the literature primarily describes the use of low-attachment methods [11–13] and agarose microwell platform [14] generating systems that allow assessment of β -cell function, including dissociation and re-aggregation of human islets of different sizes and compositions [11,12], cell lineages giving rise to pseudo-islets in 3D culture [13,14], and primary islets co-cultured with non-pancreatic cells in microfluidic devices [15]. However, methods such as magnetic bead assembly remain underexplored for endocrine pancreatic cells. On the other hand, they have been successfully used for 3D culture of human exocrine pancreatic cancer cells (human pancreatic epithelial carcinoma cell line PANC-1), aiming at drug screening [10]. Implementing an alternative 3D culture strategy for endocrine pancreas applications could provide substantial methodological advancements, particularly when combined with biologically relevant environments such as decellularized pancreatic tissue slices.

Advances in pancreatic tissue engineering have demonstrated that decellularized extracellular matrix (ECM) scaffolds offer essential biochemical and biomechanical cues that promote cell adhesion, proliferation, and differentiation, supporting the survival and function of pancreatic progenitor and β -cells [16–21]. These scaffolds have been effectively repopulated with several cell types, including mesenchymal stem cells, iPSC (induced

Pluripotent Stem Cells)-derived β -cells, and endothelial progenitor cells [22–24]. More recent approaches combine organoid formation with biomimetic scaffolds to generate a bioartificial pancreas, enhancing long-term culture, maturation, and function of endocrine cells, with promising applications not only in diabetes research but also in pancreatic cancer modeling and precision medicine platforms [2,25–29].

In the presented study, we explore the use of a magnetic bead-assisted protocol to generate 3D structures of a primary culture of human pancreatic islet cells and assess their interaction with decellularized pancreatic tissue scaffolds. While some limitations of the technique are acknowledged, our findings reveal important insights into the formation, organization, and behavior of insulin-producing 3D clusters in a biologically relevant microenvironment. These findings help advance the continuous improvement of 3D culture methodologies and provide a basis for future applications in diabetes research and tissue engineering.

2. Materials and Methods

2.1. Isolation and 2D Culture of Human Pancreatic Islets

A human pancreas from a brain-dead adult donor ($n = 1$) was obtained following Brazilian regulations and approved by the local Institutional Ethics Committee of the University of São Paulo Medical School (CEP FMUSP; CAAE 47887115.6.0000.0065; Approval Code: 2.695.463; Approval Date: 6 June 2018) for isolation and processing of pancreatic islets. Table 1 provides an overview of the donor characteristics and information for the islets used in this study. Pancreatic islets were obtained following ductal distension of the pancreas and enzymatic digestion with collagenase and neutral protease (SERVA Electrophoresis), based on Ricordi's automated method [30], with modifications [31], as previously reported [32]. In short, islet purification was performed using a continuous Ficoll density gradient on a COBE 2991 Cell Processor (Gambro, Bakersfield, CA, USA). The islet preparation used in this study yielded approximately 34,217 IEQs (Islet Equivalents, defined as islets normalized to a diameter of 150 μ m), with a purity of $70 \pm 4\%$ as determined by Dithizone staining. Cell viability was about 80%, assessed by the Live/Dead fluorescent method, based on the incorporation of fluorescein diacetate (FDA, Sigma-Aldrich, Saint Louis, MO, USA) by viable cells and propidium iodide (PI, Sigma-Aldrich, Saint Louis, MO, USA) by non-viable cells, evaluated under fluorescence microscopy. After isolation, the islets (2×10^4 islet equivalents [IEQ] per 100 cm^2 plate) were cultured as adherent cells in CMRL 1066 medium (5.6 mM glucose) (Mediatech-Cellgro, Manassas, VA, USA), supplemented with 1 mM L-glutamine (Sigma-Aldrich, Saint Louis, MO, USA), 0.2% ciprofloxacin (Sigma-Aldrich, Saint Louis, MO, USA), and 10% fetal calf serum (FCS) (Cultilab, Campinas, SP, Brazil) at 37 °C in a 5% CO_2 atmosphere. The medium was renewed every three days. Upon seeding onto adherent surface flasks or plates, the cells migrate out from each adhered pancreatic islet and spread throughout the surface [33].

Table 1. Human islets donor information.

Patient Code	Gender	Age (Years)	BMI	Blood Type	Cause of Death	Glucose (mg/dL)	Amylase (U/L)	Hb (g/dL)
P0115	Female	49	29	AB	SAH Fisher 4	164	80	14.3

BMI—body mass index. SAH—subarachnoid hemorrhage. Hb—hemoglobin.

2.2. Mycoplasma Contamination Assessment

The presence of mycoplasma contamination in human primary pancreatic islet preparations was evaluated as part of routine microbiological quality control. Detection was

performed using a nested polymerase chain reaction (Nested-PCR) method, as previously described by Uemori et al. [10]. This approach targets highly conserved sequences in the ribosomal RNA (rRNA) genes of prokaryotes, including mycoplasma species. The PCR products were examined using 2% agarose gel electrophoresis and visualized with UV illumination. A no-template negative control and a positive control were included in each run.

2.3. Cell Characterization by Immunophenotyping

Human islets' primary cultures were characterized by immunophenotyping of their membrane proteins by flow cytometry. To this end, the cells were detached from the plate using the TrypLE enzyme (Life Technologies, Carlsbad, CA, USA) and fixed with 4% paraformaldehyde (PFA) for 1 h at room temperature. Non-specific epitopes were blocked with a solution containing 5% BSA and 0.01% Triton-X and incubated for 12–16 h with primary antibodies against insulin (NewPortGreen, Invitrogen, Carlsbad, CA, USA), C-peptide (Invitrogen, Carlsbad, CA, USA), amylin (Abcam, Waltham, MA, USA), glucose transporter 2—Glut2 (Chemicon International, Temecula, CA, USA), pancreatic and duodenal homeobox 1—PDX1 (Millipore, Burlington, MA, USA), neurogenin-3—NGN3 (Millipore, Burlington, MA, USA), nestin—NES (Invitrogen, Carlsbad, CA, USA), growth factor GATA4 (Invitrogen, Carlsbad, CA, USA) and CXC chemokine receptor type 4 CXCR4 (Abcam, Waltham, MA, USA). After washing, the cultures were incubated with the respective secondary antibodies coupled to fluorophores. As a negative control, IgG1 isotypic controls coupled to the same fluorophores were used. Cell labeling was evaluated in a FACS Aria II cytometer (BD Biosciences, Franklin Lakes, NJ, USA).

2.4. Human Primary Pancreatic Islet Cells-Derived 3D Cultures

Three-dimensional (3D) cultures were established from primary human pancreatic islet cells initially grown in two-dimensional (2D) adherent cultures using the NanoShuttle™ Kit (Greiner Bio-One, Kremsmünster, Austria) magnetic 3D culture system, following the manufacturer's instructions. Briefly, the 2D islet cells were detached from the culture surface and suspended, then incubated with the NanoShuttle™ reagent-PL, containing gold, iron oxide, and poly-L-lysine nanoparticles, by centrifugation. According to the manufacturer, the nanoparticles remain attached to the cell membrane for up to eight days without affecting cell metabolism, proliferation, or inflammatory response. After nanoparticle attachment, various cell densities (0.5×10^4 – 1×10^4 and 2.5×10^4 – 5×10^4) were seeded onto non-adherent plates positioned above the magnetic base to centralize the cells and enhance their aggregation into 3D spheroids. Cultures were maintained in CMRL 1066 medium (5.6 mM glucose; Mediatech-Cellgro) supplemented with 1 mM L-glutamine (Sigma-Aldrich), 0.2% ciprofloxacin (Sigma-Aldrich), and 10% fetal calf serum (Cultilab) at 37 °C with 5% CO₂, with medium refreshed every three days.

2.5. Human Acellular Pancreatic Matrix (Bioscaffold)

A human pancreas from a brain-dead adult donor ($n = 1$) was obtained following Brazilian regulations and approved by the Institutional Ethics Committee of the University of São Paulo Medical School—CEP FMUSP (CAAE 47887115.6.0000.0065; Approval Code: 2.695.463; Approval Date: 6 June 2018) for the purpose of decellularization and the production of a pancreatic bioscaffold. This acellular human pancreatic bioscaffold was previously collected and characterized in a prior publication by our group [34]. Briefly, the pancreas was cannulated, using three blood catheters, through the pancreatic Wirsung's duct, the splenic artery, and the splenic vein. Upon cannulation, the pancreas was immediately submitted to the detergent-enzymatic decellularization protocol using 4% sodium deoxycholate (SDC) [3]. The pancreatic bioscaffold generated by decellularization was

maintained in saline phosphate buffer (PBSA) at 4 °C until ready to use. To generate the thin sections, samples of approximately 1 mm length, 1 mm width, and 1 mm thickness were included in an OCT (optimal cutting temperature) compound (Fisher HealthCare, Pittsburgh, PA, USA) and stored at −80 °C until use. For histological sectioning, the samples were transported on dry ice to a cryostat (Microm GmbH, Walldorf, Germany) and cut into slices of 25 µm, 50 µm, and 90 µm. The sections were then collected on coverslips, placed in 24-well non-adherent culture plates, and kept in PBSA at 4 °C until use.

2.6. Scanning Electron Microscopy (SEM)

Samples prepared for scanning electron microscopy (SEM) were initially fixed in 2.5% glutaraldehyde in 0.1 M PBSA (pH 7.4) for 1 h, followed by three washes in 0.1 M PBSA for 15 min each. They were then treated with 1% osmium tetroxide at 4 °C for 1 h, washed three more times in PBSA, and dehydrated through a graded ethanol series (50%, 70%, 95%, and 100%) previously filtered through a 0.22 µm filter. The dehydrated samples were dried using a K850 Critical Point Dryer (Quorum Technologies Ltd., Lewes, Germany) with carbon dioxide, mounted on copper conductive tape (3M, Maplewood, MN, USA), and coated with gold in a Desk II Sputter Coater (Denton Vacuum, Moorestown, NJ, USA) for 180 s. SEM imaging was performed using a LEO 435VP (CADI) scanning electron microscope (Zeiss, Oberkochen, Germany).

2.7. Histological Analysis

For histological analysis via optical microscopy, samples were fixed in 4% paraformaldehyde for at least 24 h and stored in 70% ethanol. Following fixation, samples were dehydrated through a graded ethanol series (70%, 96%, and 100%), cleared in xylene, and embedded in paraffin. Sections of 4–5 µm thickness were cut using a microtome and mounted on silanized slides. For hematoxylin and eosin (H&E) staining, sections were deparaffinized, rehydrated, stained with Harris Hematoxylin for 1 min 30 s, rinsed under running water for 2 min, followed by eosin staining for 12 s, then rinsed, dehydrated through ascending ethanol concentrations (70–100%), and cleared in xylene. Slides were then mounted with mounting medium and coverslips, and stored at room temperature until imaging with an Optiphot-2 Nikon optical microscope equipped with a Nikon Digital video camera Nikon DXM1200F (Nikon, Tokyo, Japan), using NIS Elements Nikon® software (v. F3.0, Nikon, Tokyo, Japan).

2.8. Insulin Assay

The supernatants collected from human primary pancreatic islet cell cultures were analyzed for insulin levels using the Elecsys Insulin Quantitative Reagent Kit (Roche®, Basel, Switzerland), following the manufacturer's instructions on the automated Cobas E 601® system (Roche®, Basel, Switzerland).

2.9. Lactate Dehydrogenase (LDH) Assay

Lactate dehydrogenase (LDH) activity was assessed in the supernatants from human primary pancreatic islet cell cultures using the reagent kit for quantitative determination of lactate dehydrogenase activity (lactate dehydrogenase kit acc. IFCC ver.2, Roche®, Basel, Switzerland), following the manufacturer's instructions on the automated Cobas E 601® system (Roche®, Basel, Switzerland).

3. Statistical Analysis

Data are presented as the mean ± SEM. Statistical differences between group means were tested by an ordinary one-way ANOVA, along with the Brown–Forsythe test for sample homogeneity. Differences were considered statistically significant at $p \leq 0.05$.

4. Results and Discussion

In this study, we hypothesized that combining magnetic bead-guided aggregation with the use of decellularized pancreatic scaffolds would support the formation of functional 3D structures from cultured primary human islet cells. Although 3D culture systems are increasingly used in endocrine pancreas research, methods such as magnetic bead assembly remain underexplored for endocrine pancreatic cells. To test our hypothesis, we evaluated how different cell inoculum densities (0.5×10^4 – 1×10^4 and 2.5×10^4 – 5×10^4) and scaffold thicknesses (50 and 90 μm) affected cluster formation, insulin production, and cytotoxicity under static culture conditions.

Pancreatic organoids are 3D cellular assemblies that partially recapitulate the architecture and cellular heterogeneity of native pancreatic tissue. However, the term “organoid” remains subject to debate, as it is sometimes erroneously used interchangeably with spheroids or islet-like clusters, which develop into 3D structures as well, but exhibit distinct cellular composition and functional characteristics. Pancreatic organoids have become valuable models for studying pancreas development [35–37], pancreatic ductal adenocarcinoma [38,39], cystic fibrosis-related pancreatic dysfunction [40], drug screening for pancreatic disorders [10,41], and functional assessment of β -cells [11–15]. Recent advances have further refined pancreatic organoid culture techniques, enhancing their physiological relevance and expanding their applications in disease modeling and regenerative medicine (for example, endocrine organoids [42] and exocrine organoids [43]).

4.1. Cell Characterization of Human 2D Pancreatic Islets Cultures

Following the establishment of primary 2D cultures of human pancreatic islets (Figure 1B), we performed a mycoplasma contamination test using a nested PCR approach. No contamination was detected in the sample used for subsequent experiments (Figure 1A).

Immunophenotyping by flow cytometry confirmed the presence of key pancreatic endocrine markers in the 2D cultures: 53.05% insulin-positive, 60.94% C-peptide-positive, 26.56% amylin-positive, and 50.33% PDX1-positive β -cells. Additionally, populations indicative of progenitor or immature phenotypes—NGN3 (54.82%), GATA4 (54.89%), and CXCR4 (65.42%)—were detected, along with 53.00% glucagon-positive α -cells and 53.55% GLUT2-positive cells (Figure 1C). This heterogeneous cell population was used without further selection for subsequent 3D cluster formation, leveraging the physiological benefits of cellular heterogeneity [44].

4.2. Generation of 3D Human Primary Pancreatic Islet Cell Cultures

Dissociated 2D primary pancreatic islet cell cultures were rapidly and reproducibly reaggregated into 3D clusters using magnetic nanoparticles. Microscopic examination showed that, after 2 h in the magnetic plate, cells from all tested cell densities self-organized into spherical structures, which became increasingly compact, with complete cluster formation observed within 18 h (Figure 2). Various cell densities (0.5×10^4 – 1×10^4 and 2.5×10^4 – 5×10^4 cells/well) were tested, all of which formed compact, stable 3D structures that remained viable after magnetic field removal.

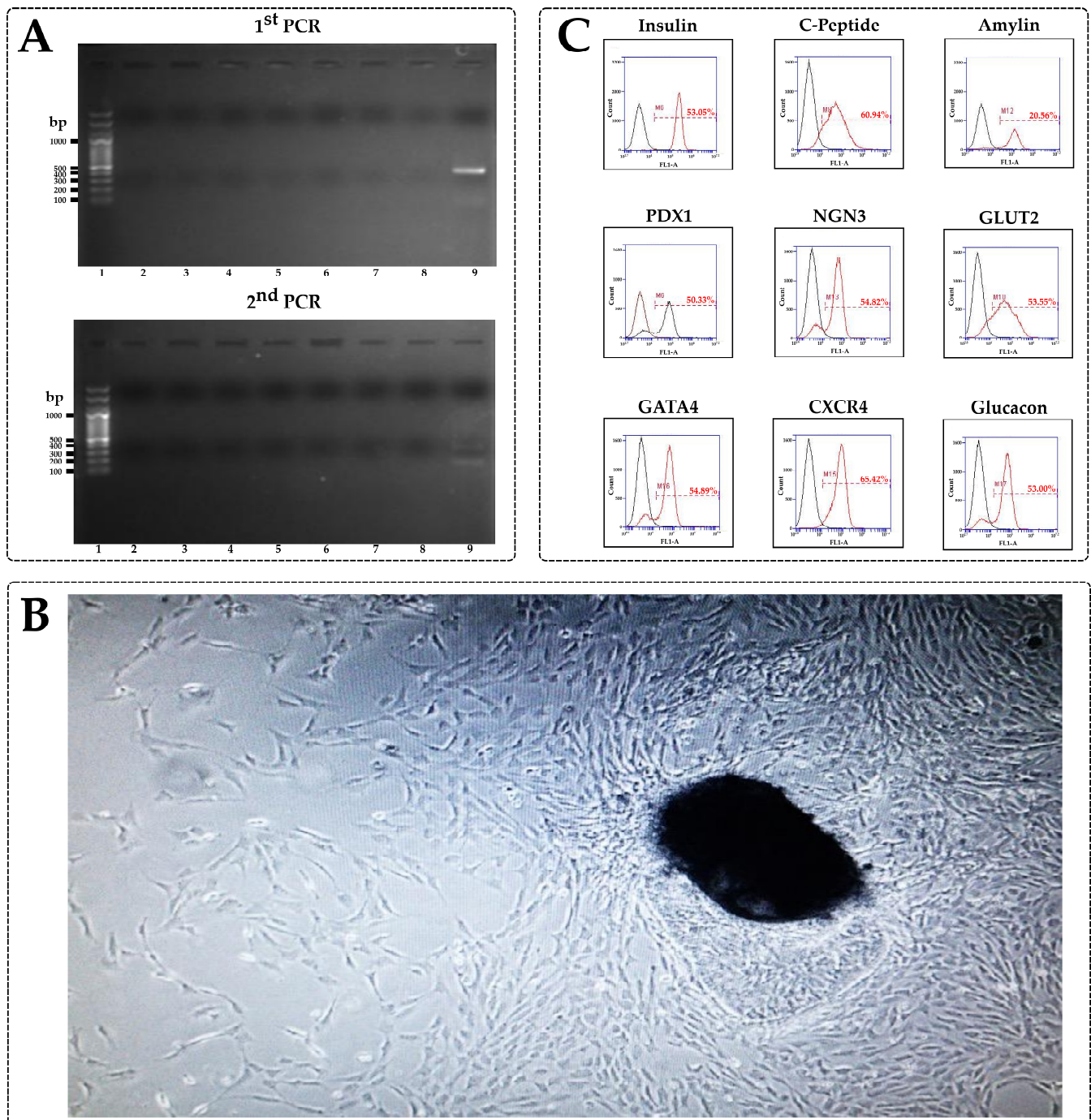


Figure 1. Cell characterization of human pancreatic islets 2D cultures. (A) Mycoplasma contamination assessment. The image shows the execution of a previously described test [45] for detecting mycoplasma contamination using the nested PCR technique. Lane 1: DNA marker; Lanes 2–7: tested samples (only lane 3 corresponds to the sample discussed in this study; other lanes represent unrelated samples run in parallel); Lane 8: Negative control (no-template control); Lane 9: Positive control. **(B) Representative image of the 2D primary culture of human pancreatic islets.** Magnification 10 \times . **(C) Immunophenotyping of the 2D culture of primary human islet cells.** Showing the following positive populations: Insulin (53.05%), C-peptide (60.94%), Amylin (26.56%), PDX1 (50.33%), NGN3 (54.82%), GLUT2 (53.55%), GATA4 (54.89%), CXCR4 (65.42%), and Glucagon (53.00%).

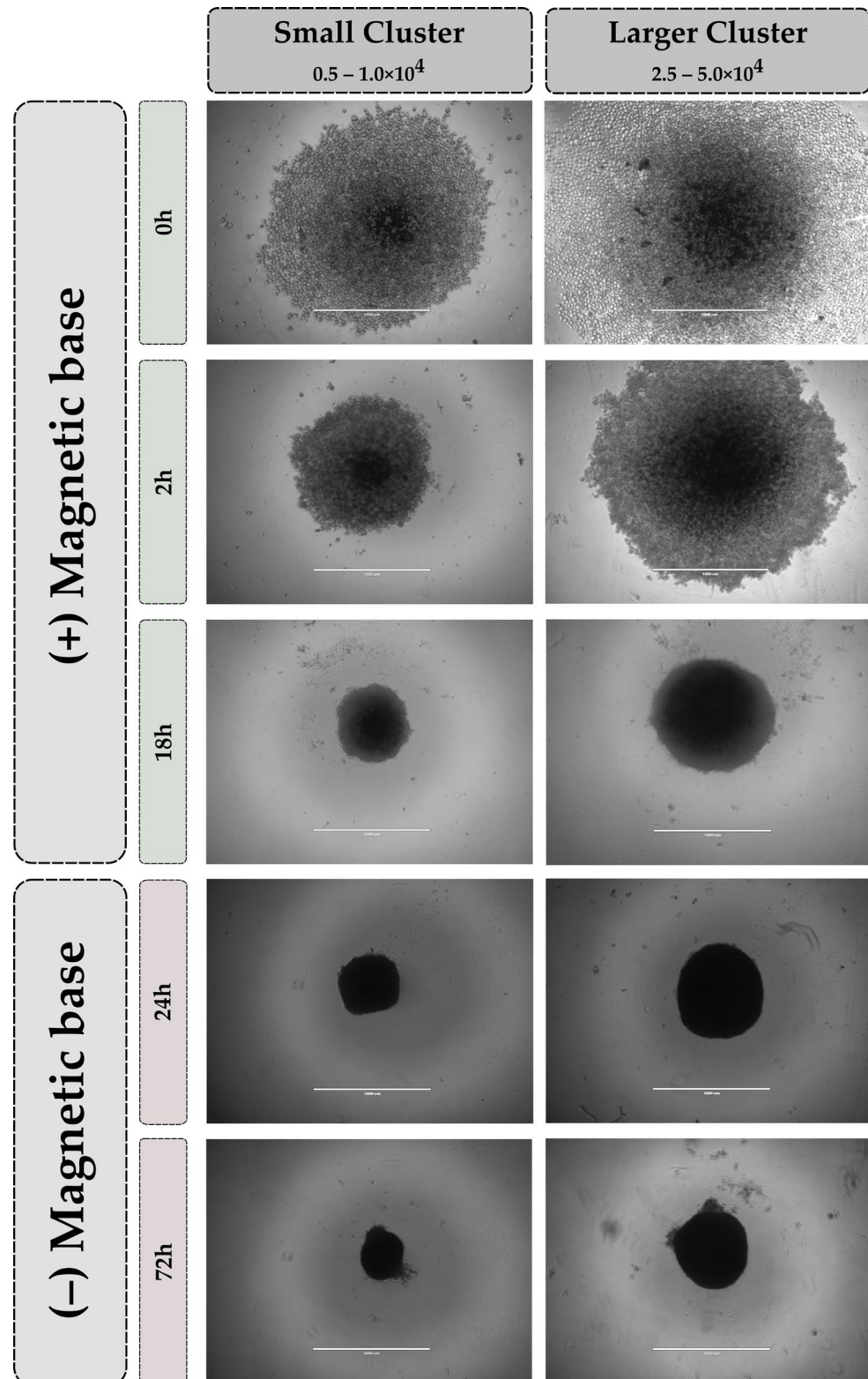


Figure 2. Human 3D primary pancreatic islet cell cultures. After impregnating the cells with the magnetic reagent, different cell numbers (0.5×10^4 – 1×10^4 and 2.5×10^4 – 5×10^4) were plated onto non-adherent plates. The figure illustrates the arrangement of 3D cultures of human primary pancreatic islet cells (structures/clusters) at two distinct stages: initially on a magnetic base at 0, 2, and 18 h, and subsequently without the magnetic base for an additional 24 and 72 h. Scale bar 1000 μ m.

Histological analysis (H&E staining) revealed 3D structures to be circular with an epithelial-like polarization outer cell layer, resembling differentiation patterns observed in epithelial spheroids [46,47], though no central lumen was detected (Figure 3). Notably, the 3D structures retained pigmentation from the magnetic nanoparticles beyond 16 days in culture, exceeding the manufacturer's expected release timeframe.

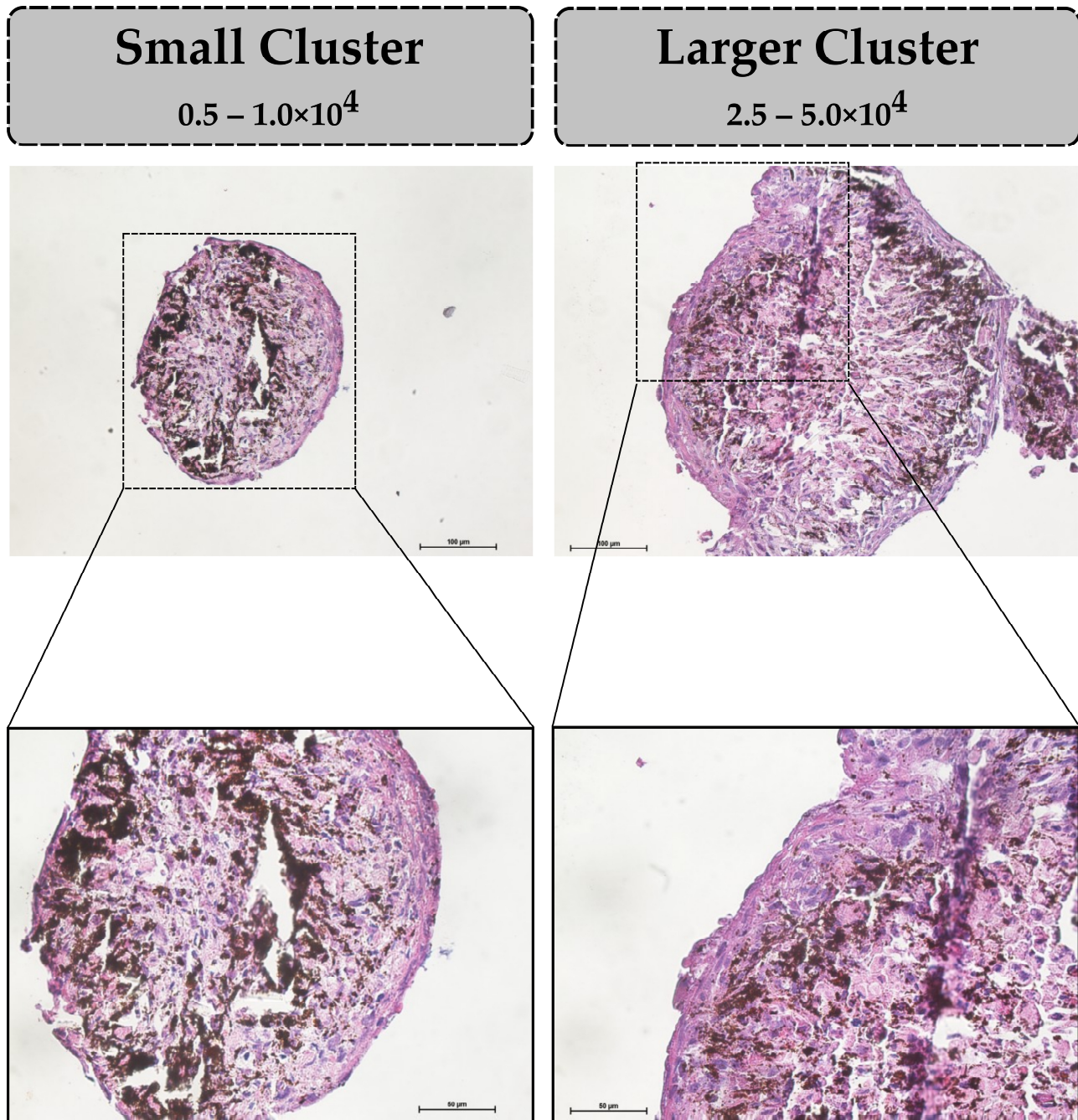


Figure 3. Histological analysis of 3D structures—Hematoxylin and eosin (H&E) staining. The figure shows the microscopic organization of the human 3D primary pancreatic islet cell cultures. Cellular self-organized spheres derived from 0.5×10^4 – 1×10^4 cells (small clusters). Scale bar 100 µm and 50 µm (zoom). Cellular self-organized spheres derived from 2.5×10^4 – 5×10^4 cells (larger clusters). Scale bar 100 µm and 50 µm (zoom). Under all conditions, it was possible to note a smooth epithelium-like surface on the 3D structures.

The magnetic bead-based method uses the NanoShuttle™ reagent-PL, composed of gold, iron oxide, and poly-L-lysine nanoparticles. As reported by the manufacturer, the

reagent stays attached to the cell membrane for up to eight days before being released into the culture medium. Notably, our findings align with previous studies indicating that poly-L-lysine-coated iron oxide nanoparticles exhibit prolonged intracellular retention. For instance, research by Babic et al. (2008) [48] demonstrated that poly-L-lysine-modified iron oxide nanoparticles were efficiently internalized by mesenchymal stem cells and retained within the cells, as confirmed by electron microscopy and Prussian blue staining. Similarly, studies by Pongrac et al. (2016) [49] reported that poly-L-lysine-coated maghemite nanoparticles were effectively utilized for neural stem cell labeling, with minimal cytotoxicity observed over extended periods of time. These findings underscore the potential of magnetic bead-assisted 3D culture systems in generating insulin-producing aggregates/spheroids/organoids and highlight the need for careful consideration of nanoparticle retention and its implications for cellular behavior and experimental outcomes.

4.3. Interaction Between 3D Clusters and the Acellular Pancreatic Bioscaffold

The results shown in Figure 4 indicate that, in the absence of an acellular pancreatic scaffold (control), the clusters derived from a smaller number of cells only attach to the plastic surface at the 6th day after plating, while larger clusters do not attach at all. When seeded onto bioscaffold slices of varying thickness, smaller 3D structures (0.5×10^4 – 1×10^4 cells) adhered to the matrix within 1–3 days, migrated into the scaffold between days 3–6, and tended to envelop and intertwine with the scaffold. In contrast, larger 3D structures (2.5×10^4 – 5×10^4 cells) exhibited delayed attachment and limited envelopment, with no visible migration observed (Figure 4).

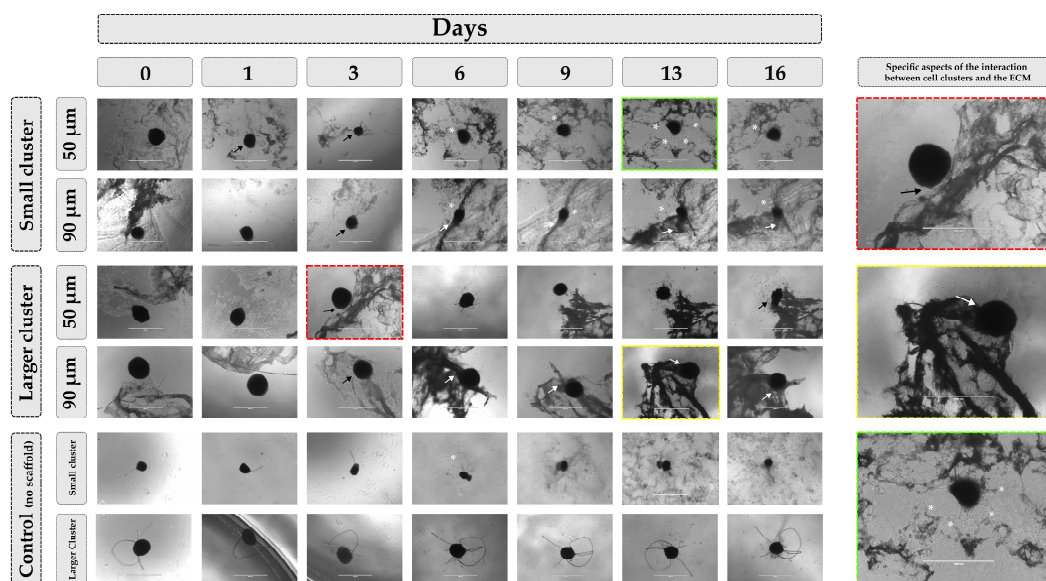


Figure 4. Three-dimensional (3D) cultures derived from human primary pancreatic islet cells (cell clusters) were seeded onto human acellular pancreatic matrix slices. Clusters generated from varying cell numbers were placed onto different thicknesses of acellular slices (0.5×10^4 – 1×10^4 cells and 2.5×10^4 – 5×10^4 cells on 50 μm and 90 μm slices) and observed at days 0, 1, 3, 6, 9, 13, and 16. Black arrows denote associations between cell structures and the bioscaffold, asterisks indicate cells adhered to the matrix, and white arrows show 3D structures being enveloped by the bioscaffold. On the right panel, the images were taken from the full panel (left). The 3D structures from the same experimental conditions were tracked throughout the experiment. ECM: extracellular matrix. Scale bar: 1000 μm .

Scanning electron microscopy (SEM), carried out at day 16, confirmed 3D clusters association with the acellular matrix and the presence of cells outside the clusters resulting from their interaction with the matrix. This SEM analysis revealed the nanofibrous structure

of the human acellular pancreatic matrix and its interaction with the clusters (Figure 5). Figure 5 shows a representative aspect of 3D smaller clusters with visible cells outside the cluster and interacting with the ECM network of the bioscaffold slice, and a representative aspect of larger 3D clusters with no visible cells outside the cluster, but a positive association with the matrix.

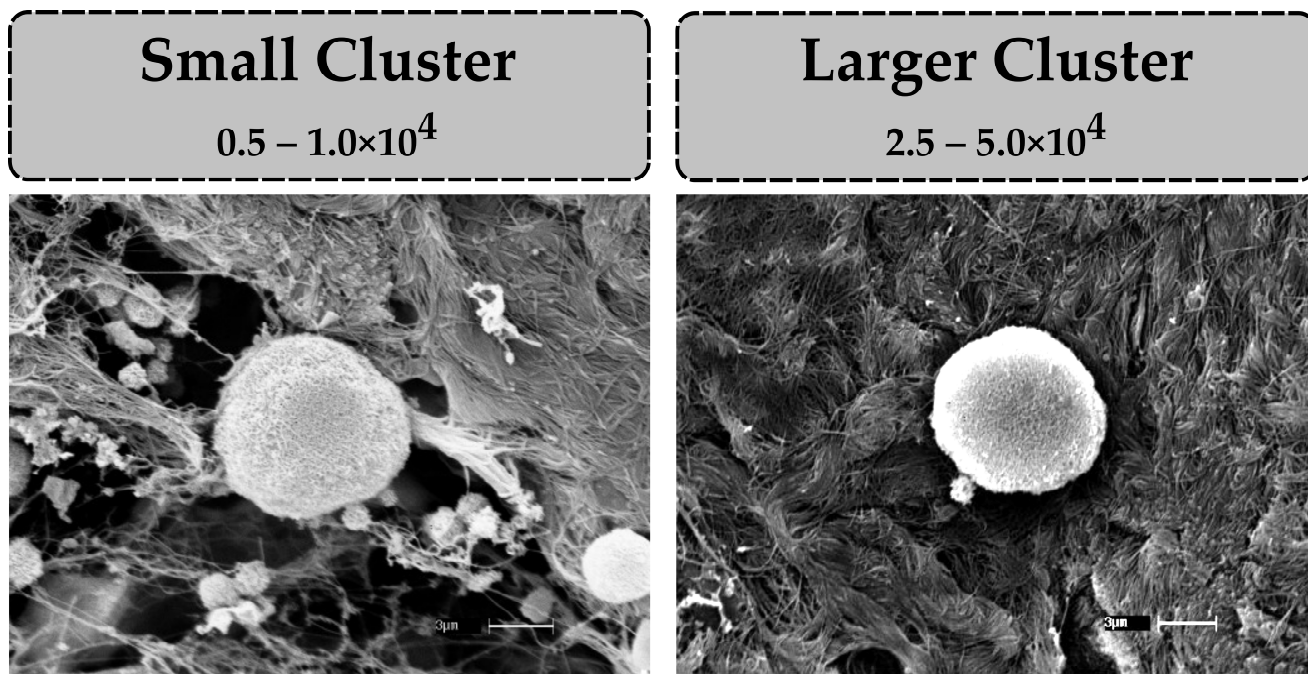


Figure 5. Scanning electron microscopy (SEM) of 3D human primary pancreatic islet cell clusters seeded on human acellular pancreatic matrix. The 3D images highlight the nanofibrous architecture of the matrix and its interaction with the cell clusters. The figure shows a representative smaller 3D cluster with cells visible outside the cluster (**left**) and a representative larger 3D cluster (**right**) with no cells visible outside, yet showing interaction with the matrix. Scale bar: 3 μm .

4.4. Functional Assessment: Insulin Secretion and Cytotoxicity

Both insulin and lactate dehydrogenase (LDH) were detected in the culture medium supernatant on the 16th day after the human 3D primary pancreatic islets cultures were seeded onto the acellular pancreatic slices. The results, displayed in Figure 6A, indicate no statistically significant difference in the levels of insulin released in the culture medium between the human primary pancreatic islet cells–derived 3D cultures alone or seeded onto the acellular pancreatic matrix (Figure 6A), indicating positive insulin secretion under all different conditions. Figure 6B indicates no statistically significant difference in the levels of LDH released to the culture medium when comparing the human 3D primary pancreatic islets cultures alone or seeded onto the acellular pancreatic matrix. However, larger 3D structures displayed slightly higher accumulated LDH values, when compared to the smaller ones (Figure 6B), which can be due to the larger number of cells present in these clusters, indicating an increased cellular turnover or cell death caused by lower oxygenation of the clusters' inner region [50].

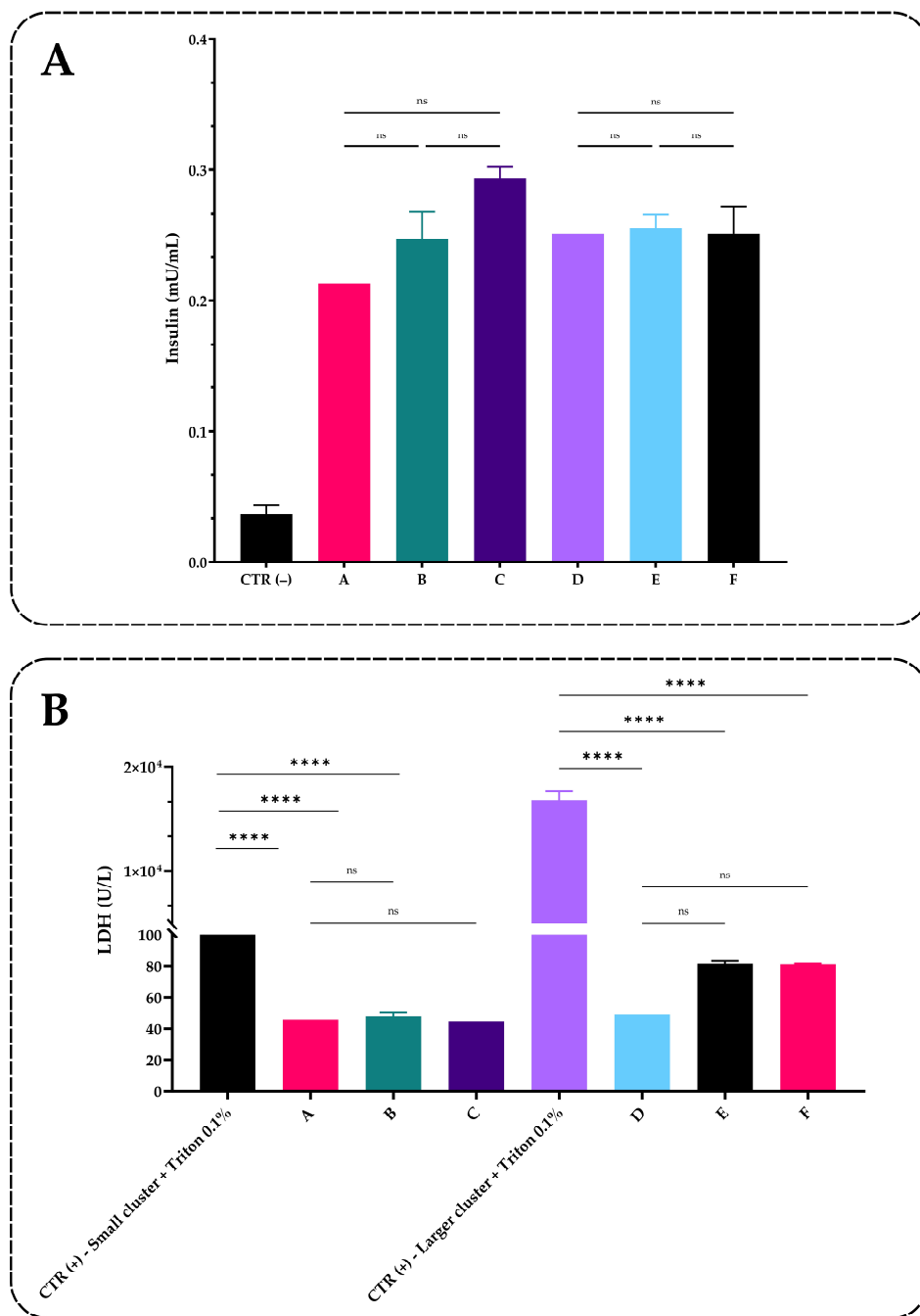


Figure 6. Analysis of insulin and lactate dehydrogenase (LDH) levels. These assays were performed using the culture medium collected on the 16th day after the human primary pancreatic islets-derived 3D clusters were cultured onto acellular pancreatic slices. (A) represents insulin quantification (mU/mL). CTR (-) Culture medium (negative control); (A) 3D representative small cluster (0.5×10^4 – 1×10^4 cells)—no scaffold; (B) 3D small cluster derived from 0.5×10^4 – 1×10^4 cells seeded onto 50 μ m acellular matrix slice; (C) 3D small cluster derived from 0.5×10^4 – 1×10^4 cells seeded onto 90 μ m acellular matrix slice; (D) 3D representative larger cluster (2.5×10^4 – 5×10^4 cells)—no scaffold; (E) 3D larger cluster derived from 2.5×10^4 – 5×10^4 cells seeded onto 50 μ m acellular matrix slice; (F) 3D larger cluster derived from 2.5×10^4 – 5×10^4 cells seeded onto 90 μ m acellular matrix slice; (B) represents LDH quantification (U/L). CTR (+) Small cluster (0.5×10^4 – 1×10^4 cells) + Triton X-100 0.1% (positive control); (A) 3D representative small cluster (0.5×10^4 – 1×10^4 cells)—no scaffold; (B) 3D small cluster derived from 0.5×10^4 – 1×10^4 cells seeded onto 50 μ m acellular matrix slice; (C) 3D small cluster derived from 0.5×10^4 – 1×10^4 cells seeded onto 90 μ m acellular matrix slice; CTR (+) Larger cluster (2.5×10^4 – 5×10^4 cells) + Triton X-100 0.1% (positive control); (D) 3D representative larger cluster (2.5×10^4 – 5×10^4 cells)—no scaffold; (E) 3D larger cluster derived from

2.5×10^4 – 5×10^4 cells seeded onto 50 μm acellular matrix slice; (F) 3D larger cluster derived from 2.5×10^4 – 5×10^4 cells seeded onto 90 μm acellular matrix slice. Data are presented as the mean value \pm SEM (standard error of mean) in triplicate. The statistical analysis was made by an ordinary one-way ANOVA using mixed multiple comparisons. **** ≤ 0.0001 ; ns: no statistically significant difference. All analyses were made with GraphPad Prism (v. 10.6.1).

5. Conclusions

Several three-dimensional (3D) culture models have been developed for studying the endocrine pancreas, each with distinct approaches and limitations. Unlike many existing systems, we employed the magnetic bead-based model for the first time in the context of endocrine pancreatic cells. We started with dissociated human pancreatic islet cells cultured in 2D, a condition under which they adhere to the plastic surface and lose their native architecture. Using a magnetic bead-assisted method (NanoShuttle™), the cells were reaggregated into 3D pseudo-islets, whose size and cellular composition can potentially be controlled. The resulting 3D structures exhibit a circular morphology with a polarized epithelial-like outer layer, although they do not develop a central lumen.

Importantly, these 3D structures can be co-cultured with acellular human pancreatic bioscaffolds, which provide not only structural support and spatial orientation but also biochemical cues that promote cell adhesion and potentially enhance functionality. We observed differential behavior between the smaller and larger 3D structures: smaller clusters adhered more efficiently to the bioscaffold slices and exhibited migratory behavior and integration into the matrix, while larger clusters showed delayed attachment and no visible migration. These observations, along with slightly elevated LDH levels in larger structures, highlight the importance of cluster size in scaffold integration and further support the use of a decellularized matrix to create a tissue-relevant microenvironment for physiologically meaningful studies.

Nevertheless, considering the advantages and limitations of magnetic bead-based 3D culture systems, the choice of methodology for generating three-dimensional cultures of insulin-producing cells ultimately depends on the specific goals and criteria of the researcher. Careful evaluation of each protocol's suitability, based on factors such as cell type, functionality, reproducibility, and potential side effects, is essential. Despite these challenges, the ability to reproducibly generate functional endocrine clusters and assess their behavior within a tissue-relevant microenvironment highlights the potential of this approach as a platform for studying pancreatic physiology and advancing diabetes research.

Author Contributions: M.d.C.M. designed the study, accepted the human pancreas donation offered to the NUCEL group based on analysis of the profile of multiple organ donors, performed the human islet isolation and decellularization, cultured human islets in 2D and 3D models, carried out the characterization assays, performed the acellular pancreatic matrix characterization assays, analyzed the data and drafted the manuscript; A.C.O.C. participated of the study design, performed and analyzed the SEM assay and reviewed the manuscript; N.R.D.-R. performed the histological characterization of acellular pancreatic matrices and clusters and reviewed the manuscript; E.G.C. contributed to the conception of the study, supervised the histological characterization of the acellular pancreatic matrix, participated in data interpretation, and critically reviewed the manuscript for important intellectual content; M.C.S. contributed to the conception and design of the study, supervised its execution, participated in data analysis and interpretation, and critically reviewed and edited the manuscript. All authors have read and agreed to the published version of the manuscript.

Funding: This work was supported by grants from the following Brazilian research agencies: BNDES, CAPES (PVE process number 88881.068070/2014-01), CNPq (grant numbers 457601/2013-2 and

401430/2013-8), FAPESP (Thematic grant number 2016/05311-2), FINEP, and the Ministries of Science and Technology (MCTI) and Health (MS-DECIT).

Institutional Review Board Statement: The study was conducted in accordance with the Brazilian regulations and approved by the local Institutional Ethics Committee of the University of São Paulo Medical School (CEP FMUSP; CAAE 47887115.6.0000.0065; Approval Code: 2.695.463; Approval Date: 6 June 2018).

Informed Consent Statement: Informed consent for participation was replaced by a Deceased Donor Organ and Tissue Donation Term, signed by the donor's family, in accordance with Brazilian regulations and approved by the local Institutional Ethics Committee of the University of São Paulo Medical School (CEP FMUSP; CAAE 47887115.6.0000.0065; Approval Code: 2.695.463; Approval Date: 6 June 2018).

Data Availability Statement: The original contributions presented in this study are included in the article. Further inquiries can be directed to the corresponding author.

Acknowledgments: We are especially grateful to the excellent technical assistance provided by Zizi de Mendonça, LIM-59 (FM-USP) and the Advanced Center for Diagnostics by Images of the University of São Paulo Veterinary School of Medicine (CADI-FMVZ-USP) and also to Henrique Capistrano-Melo (Graduate Program in Experimental Physiopathology, School of Medicine, Universidade de São Paulo) and to Leandro Teodoro Júnior (Instituto de Química, Universidade de São Paulo) for help with the quality formatting of the figures.

Conflicts of Interest: The authors declare no conflict of interest.

References

1. Diane, A.; Mohammed, L.I.; Al-Siddiqi, H.H. Islets in the body are never flat: Transitioning from two-dimensional (2D) monolayer culture to three-dimensional (3D) spheroid for better efficiency in the generation of functional hPSC-derived pancreatic β cells in vitro. *Cell Commun. Signal.* **2023**, *21*, 151. [CrossRef] [PubMed] [PubMed Central]
2. Moreira, L.; Bakir, B.; Chatterji, P.; Dantes, Z.; Reichert, M.; Rustgi, A.K. Pancreas 3D Organoids: Current and Future Aspects as a Research Platform for Personalized Medicine in Pancreatic Cancer. *Cell. Mol. Gastroenterol. Hepatol.* **2018**, *5*, 289–298. [CrossRef]
3. Bakhti, M.; Bottcher, A.; Lickert, H. Modelling the endocrine pancreas in health and disease. *Nat. Rev. Endocrinol.* **2019**, *15*, 155–171. [CrossRef]
4. Pollock, S.D.; Galicia-Silva, I.M.; Liu, M.; Gruskin, Z.L.; Alvarez-Dominguez, J.R. Scalable Generation of 3D Pancreatic Islet Organoids from Human Pluripotent Stem Cells in Suspension Bioreactors. In *Tissue Morphogenesis: Methods in Molecular Biology*; Nelson, C.M., Ed.; Humana: New York, NY, USA, 2024; Volume 2805. [CrossRef]
5. Vandana, J.J.; Manrique, C.; Lacko, L.A.; Chen, S. Human pluripotent-stem-cell-derived organoids for drug discovery and evaluation. *Cell Stem Cell* **2023**, *30*, 571–591. [CrossRef] [PubMed] [PubMed Central]
6. Bialkowska, K.; Komorowski, P.; Bryszewska, M.; Milowska, K. Spheroids as a type of three-dimensional cell cultures—Examples of methods of preparation and the most important application. *Int. J. Mol. Sci.* **2020**, *21*, 6225. [CrossRef]
7. Razian, G.; Yu, Y.; Ungrin, M. Production of large numbers of size-controlled tumor spheroids using microwell plates. *J. Vis. Exp.* **2013**, *81*, e50665. [PubMed]
8. Napolitano, A.P.; Dean, D.M.; Man, A.J.; Youssef, J.; Ho, D.N.; Rago, A.P.; Lech, M.P.; Morgan, J.R. Scaffold-free three-dimensional cell culture utilizing micromolded nonadhesive hydrogels. *Biotechniques* **2007**, *43*, 496–500. [CrossRef] [PubMed]
9. Andersen, T.; Auk-Emblem, P.; Dornish, M. 3D Cell culture in alginate hydrogels. *Microarrays* **2015**, *4*, 133–161. [CrossRef]
10. Hou, S.; Tiriach, H.; Sridharan, B.P.; Scampavia, L.; Madoux, F.; Seldin, J.; Souza, G.R.; Watson, D.; Tuveson, D.; Spicer, T.P. Advanced development of primary pancreatic organoid tumor models for high-throughput phenotypic drug screening. *SLAS Discov.* **2018**, *23*, 574–584. [CrossRef] [PubMed]
11. Halban, P.A.; Powers, S.L.; George, K.L.; Bonner-Weir, S. Spontaneous reassociation of dispersed adult rat pancreatic islet cells into aggregates with three-dimensional architecture typical of native islets. *Diabetes* **1987**, *36*, 783–790. [CrossRef]
12. Quesada-Masachs, E.; Zilberman, S.; Rajendran, S.; Chu, T.; McArdle, S.; Kiosses, W.B.; Lee, J.M.; Yesildag, B.; Benkahla, M.A.; Pawlowska, A.; et al. Upregulation of HLA class II in pancreatic beta cells from organ donors with type 1 diabetes. *Diabetologia* **2022**, *65*, 387–401. [CrossRef] [PubMed]
13. Lecomte, M.J.; Pechberty, S.; Machado, C.; Da Barroca, S.; Ravassard, P.; Scharfmann, R.; Czernichow, P.; Duvillie, B. Aggregation of Engineered Human beta-Cells Into Pseudoislets: Insulin Secretion and Gene Expression Profile in Normoxic and Hypoxic Milieu. *Cell Med.* **2016**, *8*, 99–112. [CrossRef] [PubMed]

14. Skrzypek, K.; Barrera, Y.B.; Groth, T.; Stamatialis, D. Endothelial and beta cell composite aggregates for improved function of a bioartificial pancreas encapsulation device. *Int. J. Artif. Organs* **2018**, *41*, 152–159. [[CrossRef](#)]
15. Sankar, K.S.; Green, B.J.; Crocker, A.R.; Verity, J.E.; Altamentova, S.M.; Rocheleau, J.V. Culturing pancreatic islets in microfluidic flow enhances morphology of the associated endothelial cells. *PLoS ONE* **2011**, *6*, e24904. [[CrossRef](#)]
16. Brown, B.N.; Barnes, C.A.; Kasick, R.T.; Michel, R.; Gilbert, T.W.; Beer-Stolz, D.; Castner, D.G.; Ratner, B.D.; Badylak, S.F. Surface characterization of extracellular matrix scaffolds. *Biomaterials* **2010**, *31*, 428–437. [[CrossRef](#)]
17. Gilbert, T.W.; Sellaro, T.L.; Badylak, S.F. Decellularization of tissues and organs. *Biomaterials* **2006**, *27*, 3675–3683. [[CrossRef](#)]
18. Cortiella, J.; Niles, J.; Cantu, A.; Brettler, A.; Pham, A.; Vargas, G.; Winston, S.; Wang, J.; Walls, S.; Nichols, J.E. Influence of acellular natural lung matrix on murine embryonic stem cell differentiation and tissue formation. *Tissue Eng. Part A* **2010**, *16*, 2565–2580. [[CrossRef](#)]
19. Sellaro, T.L.; Ranade, A.; Faulk, D.M.; McCabe, G.P.; Dorko, K.; Badylak, S.F.; Strom, S.C. Maintenance of human hepatocyte function in vitro by liver-derived extracellular matrix gels. *Tissue Eng. Part A* **2010**, *16*, 1075–1082. [[CrossRef](#)]
20. Valentin, J.E.; Turner, N.J.; Gilbert, T.W.; Badylak, S.F. Functional skeletal muscle formation with a biologic scaffold. *Biomaterials* **2010**, *31*, 7475–7484. [[CrossRef](#)] [[PubMed](#)]
21. Youngblood, R.L.; Sampson, J.P.; Lebioda, K.R.; Shea, L.D. Microporous scaffolds support assembly and differentiation of pancreatic progenitors into β -cell clusters. *Acta Biomater.* **2019**, *96*, 111–122. [[CrossRef](#)] [[PubMed](#)] [[PubMed Central](#)]
22. De Carlo, E.; Baiguera, S.; Conconi, M.T.; Vigolo, S.; Grandi, C.; Lora, S.; Martini, C.; Maffei, P.; Tamagno, G.; Vettor, R.; et al. Pancreatic acellular matrix supports islet survival and function in a synthetic tubular device: In vitro and in vivo studies. *Int. J. Mol. Med.* **2010**, *25*, 195–202. [[CrossRef](#)]
23. Goh, S.K.; Bertera, S.; Olsen, P.; Candiello, J.E.; Halfter, W.; Uechi, G.; Balasubramani, M.; Johnson, S.A.; Sicari, B.M.; Kollar, E.; et al. Perfusion-decellularized pancreas as a natural 3D scaffold for pancreatic tissue and whole organ engineering. *Biomaterials* **2013**, *34*, 6760–6772. [[CrossRef](#)]
24. Guo, Y.; Wu, C.; Xu, L.; Xu, Y.; Li, X.; Zhu, H.; Lu, J.; Lu, Y.; Wang, Z. Vascularization of pancreatic decellularized scaffold with endothelial progenitor cells. *J. Artif. Organs Off. J. Jpn. Soc. Artif. Organs* **2018**, *21*, 230–237. [[CrossRef](#)]
25. Napierala, H.; Hillebrandt, K.H.; Haep, N.; Tang, P.; Tintemann, M.; Gassner, J.; Noesser, M.; Everwien, H.; Seiffert, N.; Kluge, M.; et al. Engineering an endocrine Neo-Pancreas by repopulation of a decellularized rat pancreas with islets of Langerhans. *Sci. Rep.* **2017**, *7*, 41777. [[CrossRef](#)]
26. Peloso, A.; Urbani, L.; Cravedi, P.; Katari, R.; Maghsoudlou, P.; Fallas, M.E.; Sordi, V.; Citro, A.; Purroy, C.; Niu, G.; et al. The Human Pancreas as a Source of Protolerogenic Extracellular Matrix Scaffold for a New-generation Bioartificial Endocrine Pancreas. *Ann. Surg.* **2016**, *264*, 169–179. [[CrossRef](#)] [[PubMed](#)]
27. Wang, X.; Li, Y.G.; Du, Y.; Zhu, J.Y.; Li, Z. The Research of Acellular Pancreatic Bioscaffold as a Natural 3-Dimensional Platform In Vitro. *Pancreas* **2018**, *47*, 1040–1049. [[CrossRef](#)] [[PubMed](#)]
28. Hakobyan, D.; Médina, C.; Dusserre, N.; Stachowicz, M.L.; Handschin, C.; Fricain, J.C.; Guillermet-Guibert, J.; Oliveira, H. Laser-assisted 3D bioprinting of exocrine pancreas spheroid models for cancer initiation study. *Biofabrication* **2020**, *12*, 035001. [[CrossRef](#)] [[PubMed](#)]
29. Sá, J.; Sá, S.; Leménager, H.; Costa, R.; Onteniente, B.; Soares, R.; Ribeiro, V.P.; Oliveira, A.L. Advancing diabetes treatment: From human beta cell technology to bioartificial pancreas development. *Front. Biomater. Sci.* **2025**, *4*, 1524518. [[CrossRef](#)]
30. Ricordi, C.; Lacy, P.E.; Finke, E.H.; Olack, B.J.; Scharp, D.W. Automated method for isolation of human pancreatic islets. *Diabetes* **1988**, *37*, 413–420. [[CrossRef](#)]
31. Shapiro, A.M.; Lakey, J.R.; Ryan, E.A.; Korbitt, G.S.; Toth, E.; Warnock, G.L.; Kneteman, N.M.; Rajotte, R.V. Islet transplantation in seven patients with type 1 diabetes mellitus using a glucocorticoid-free immunosuppressive regimen. *N. Engl. J. Med.* **2000**, *343*, 230–238. [[CrossRef](#)]
32. Labriola, L.; Montor, W.R.; Krogh, K.; Lojudice, F.H.; Genzini, T.; Goldberg, A.C.; Eliaschewitz, F.G.; Sogayar, M.C. Beneficial effects of prolactin and laminin on human pancreatic islet-cell cultures. *Mol. Cell. Endocrinol.* **2007**, *263*, 120–133. [[CrossRef](#)]
33. Phelps, E.A.; Cianciaruso, C.; Santo-Domingo, J.; Pasquier, M.; Galliverti, G.; Piemonti, L.; Berishvili, E.; Burri, O.; Wiederkehr, A.; Hubbell, J.A.; et al. Advances in pancreatic islet monolayer culture on glass surfaces enable super-resolution microscopy and insights into beta cell ciliogenesis and proliferation. *Sci. Rep.* **2017**, *7*, 45961, Erratum in: *Sci. Rep.* **2017**, *7*, 46801. <https://doi.org/10.1038/srep46801>. [[CrossRef](#)] [[PubMed](#)] [[PubMed Central](#)]
34. Mantovani, M.C.; Damaceno-Rodrigues, N.R.; Ronatty, G.T.S.; Segovia, R.S.; Pantanali, C.A.; Rocha-Santos, V.; Caldini, E.G.; Sogayar, M.C. Which detergent is most suitable for the generation of an acellular pancreas bioscaffold? *Braz. J. Med Biol. Res.* **2024**, *57*, e13107. [[CrossRef](#)] [[PubMed](#)] [[PubMed Central](#)]
35. Grapin-Botton, A. Three-dimensional pancreas organogenesis models. *Diabetes Obes. Metab.* **2016**, *18*, 33–40. [[CrossRef](#)]
36. Greggio, C.; Franceschi, F.D.; Grapin-Botton, A. Concise reviews: In vitro-produced pancreas organogenesis models in three dimensions: Self-organization from few stem cells or progenitors. *Stem Cells* **2015**, *33*, 8–14. [[CrossRef](#)] [[PubMed](#)]

37. Balak, J.R.A.; Juksar, J.; Carlotti, F.; Nigro, A.L.; de Koning, E.J.P. Organoids from the human fetal and adult pancreas. *Curr. Diabetes Rep.* **2019**, *19*, 160. [[CrossRef](#)]
38. Baker, L.A.; Tiriach, H.; Clevers, H.; Tuveson, D.A. Modeling pancreatic cancer with organoids. *Trends Cancer* **2016**, *2*, 176–190. [[CrossRef](#)]
39. Boj, S.F.; Hwang, C.-I.; Baker, L.A.; Chiol, I.I.C.; Engle, D.D.; Corbo, V.; Jager, M.; Ponz-Sarvisé, M.; Tiriach, H.; Spector, M.S.; et al. Organoid models of human and mouse ductal pancreatic cancer. *Cell* **2015**, *160*, 324–338. [[CrossRef](#)] [[PubMed](#)]
40. Hohwieler, M.; Illing, A.; Hermann, P.C.; Mayer, T.; Stockmann, M.; Perkhof, L.; Eiseler, T.; Antony, J.S.; Müller, M.; Renz, S.; et al. Human pluripotent stem cell-derived acinar/ductal organoids generate human pancreas upon orthotopic transplantation and allow disease modelling. *Gut* **2017**, *66*, 473. [[CrossRef](#)]
41. Walsh, A.J.; Castellanos, J.A.; Nagathihalli, N.S.; Merchant, N.B.; Skala, M.C. Optical imaging of drug-induced metabolism changes in murine and human pancreatic cancer organoids reveals heterogeneous drug response. *Pancreas* **2016**, *45*, 863–869. [[CrossRef](#)] [[PubMed](#)]
42. Zhang, X.; Ma, Z.; Song, E.; Xu, T. Islet organoid as a promising model for diabetes. *Protein Cell* **2022**, *13*, 239–257. [[CrossRef](#)] [[PubMed](#)] [[PubMed Central](#)]
43. Xu, J.; Pham, M.D.; Corbo, V.; Ponz-Sarvisé, M.; Oni, T.; Öhlund, D.; Hwang, C.I. Advancing pancreatic cancer research and therapeutics: The transformative role of organoid technology. *Exp. Mol. Med.* **2025**, *57*, 50–58. [[CrossRef](#)] [[PubMed](#)] [[PubMed Central](#)]
44. Rutter, G.A.; Gresch, A.; Delgadillo Silva, L.; Benninger, R.K.P. Exploring pancreatic beta-cell subgroups and their connectivity. *Nat. Metab.* **2024**, *6*, 2039–2053. [[CrossRef](#)] [[PubMed](#)]
45. Uemori, T.; Asada, K.; Kato, I.; Harasawa, R. Amplification of the 16S-23S Spacer Region in rRNA Operons of Mycoplasmas by the Polymerase Chain Reaction. *System. Appl. Microbiol.* **1992**, *15*, 181–186. [[CrossRef](#)]
46. O'Brien, L.E.; Zegers, M.M.; Mostov, K.E. Opinion: Building epithelial architecture: Insights from three-dimensional culture models. *Nat. Rev. Mol. Cell Biol.* **2002**, *3*, 531–537. [[CrossRef](#)] [[PubMed](#)]
47. Lin, R.Z.; Chou, L.F.; Chien, C.C.; Chang, H.Y. Dynamic analysis of hepatoma spheroid formation: Roles of E-cadherin and beta1-integrin. *Cell Tissue Res.* **2006**, *324*, 411–422. [[CrossRef](#)] [[PubMed](#)]
48. Babic, M.; Horák, D.; Trchová, M.; Jendelová, P.; Glogarová, K.; Lesný, P.; Herynek, V.; Hájek, M.; Syková, E. Poly(L-lysine)-modified iron oxide nanoparticles for stem cell labeling. *Bioconjug. Chem.* **2008**, *19*, 740–750. [[CrossRef](#)] [[PubMed](#)]
49. Pongrac, I.M.; Dobrivojević, M.; Ahmed, L.B.; Babič, M.; Šlouf, M.; Horák, D.; Gajović, S. Improved biocompatibility and efficient labeling of neural stem cells with poly(L-lysine)-coated maghemite nanoparticles. *Beilstein J. Nanotechnol.* **2016**, *7*, 926–936. [[CrossRef](#)] [[PubMed](#)] [[PubMed Central](#)]
50. Castiglione, H.; Madrange, L.; Lemonnier, T.; Deslys, J.-P.; Yates, F.; Vigneron, P.-A. Development and Optimization of a Lactate Dehydrogenase Assay Adapted to 3D Cell Cultures. *Organoids* **2024**, *3*, 113–125. [[CrossRef](#)]

Disclaimer/Publisher's Note: The statements, opinions and data contained in all publications are solely those of the individual author(s) and contributor(s) and not of MDPI and/or the editor(s). MDPI and/or the editor(s) disclaim responsibility for any injury to people or property resulting from any ideas, methods, instructions or products referred to in the content.